



Preparation and optical characteristics of layered perovskite-type lead-bromide-incorporated azobenzene chromophores

Ryo Sasai*, Hisashi Shinomura

Department of Applied Chemistry, Graduate School of Engineering, Nagoya University, F3-3(250), Furo-cho, Chikusa-ku, Nagoya 464-8603, Japan

ARTICLE INFO

Article history:

Received 27 July 2012

Received in revised form

6 November 2012

Accepted 11 November 2012

Available online 22 November 2012

Keywords:

Lead bromide-based layered perovskite

Azobenzene derivatives

Photoisomerization

Inorganic/organic hybrid materials

Photoluminescence

ABSTRACT

Lead bromide-based layered perovskite powders with azobenzene derivatives were prepared by a homogeneous precipitation method. From the diffuse reflectance (DR) and photoluminescence (PL) spectra of the hybrid powder materials, the present hybrids exhibited sharp absorption and PL peaks originating from excitons produced in the PbBr_2 layer. When the present hybrid powder was irradiated with UV light at 350 nm, the absorption band from the *trans*-azobenzene chromophore, observed around 350 nm, decreased, while the absorption band from the *cis*-azobenzene chromophore, observed around 450 nm, increased. These results indicate that azobenzene chromophores in the present hybrid materials exhibit reversible photoisomerization. Moreover, it was found that the PL intensity from the exciton also varied due to photoisomerization of the azobenzene chromophores in the present hybrid. Thus, for the first time we succeeded in preparing the azobenzene derivative lead-bromide-based layered perovskite with photochromism before and after UV light irradiation.

© 2012 Elsevier Inc. All rights reserved.

1. Introduction

Metal halide-based layered perovskites with chemical formulas such as $(\text{R-NH}_3)_2\text{MX}_4$ (R-NH₃: organic ammonium such as alkylammonium; M: Pb, Sn, Ge, and so on; and X: Cl, Br, and I) is well known as one of the natural two-dimensional (2D) superlattice compounds [1–16]. A strong quantum-confinement effect appears in the 2D semiconductor layer, and then a stable exciton with a large binding energy of several hundred meV is formed. As a result, metal halide-based layered perovskites exhibit attractive optical properties such as photoluminescence (PL), electroluminescence (EL), and nonlinear optical effects originating from these excitons. In earlier studies, halide-based layered perovskites that used simple alkyl ammonium molecules as organic ammonium ions were investigated [4,6,14]. In this hybrid system, organic ammonium plays only the role of an insulating barrier layer. Recently, various halide-based layered perovskite materials with not only simple alkylammonium cations but also with various functional organic ammonium ions such as chromophores, polymers, and compounds with π -conjugated systems have been reported [2,3,10,15,16]. In these reported hybrid systems, unique optical, electronic, and magnetic properties could be observed. These experimental facts indicate that the properties of these

types of hybrid systems can be controlled by using selected functional organic ammonium as cations.

It is well known that the azobenzene chromophores exhibit reversible photoisomerization from *trans*- to *cis*- forms, enabling the optical and electronic properties of azobenzene chromophores to be significantly varied by the same photoisomerization process. Thus, the photoswitching of various properties and functions by the photoisomerization of azobenzene chromophores has been attempted by many researchers [18–23]. Halide-based layered perovskites with azobenzene chromophores have also been investigated, and a photoinduced energy transfer from the *trans*-azobenzene chromophore to a lead halide semiconductor layer was reported [8,16,17]. However, photoisomerization of azobenzene chromophores and changes to the optical and/or electronic properties of a metal halide semiconductor layer by photoisomerization is yet to be achieved. In this study, we attempted to synthesize a lead-bromide-based layered perovskite, which is a typical compounds, with azobenzene ammonium derivatives, and the spectroscopic characteristics of the synthesized hybrid powder was investigated both before and after UV and/or visible light irradiation.

2. Experimental

2.1. Materials

Lead(II) bromide (Kojundo Chemical Laboratory Co., Ltd.), 4-(phenylazo)phenol (Sigma-Aldrich Co. LLC.), *n*-dibromoalkane

* Corresponding author. Present address: Department of Physics and Materials Science, Interdisciplinary Graduate School of Science and Engineering, Shimane University, 1060, Nishikawatsu-cho, Matue 690-8504, Japan.

E-mail address: rsasai@riko.shimane-u.ac.jp (R. Sasai).

(TCI), and potassium phthalimide and hydrobromic acid (Nacal Tesque) were all used without further purification. Hydrazine monohydrate, silver nitrate aqueous solution, *N,N*-dimethylformamide (DMF), and sodium hydroxide were purchased from Kishida Chemical Co., Ltd. and also used without further purification. All other solvents were reagent grade.

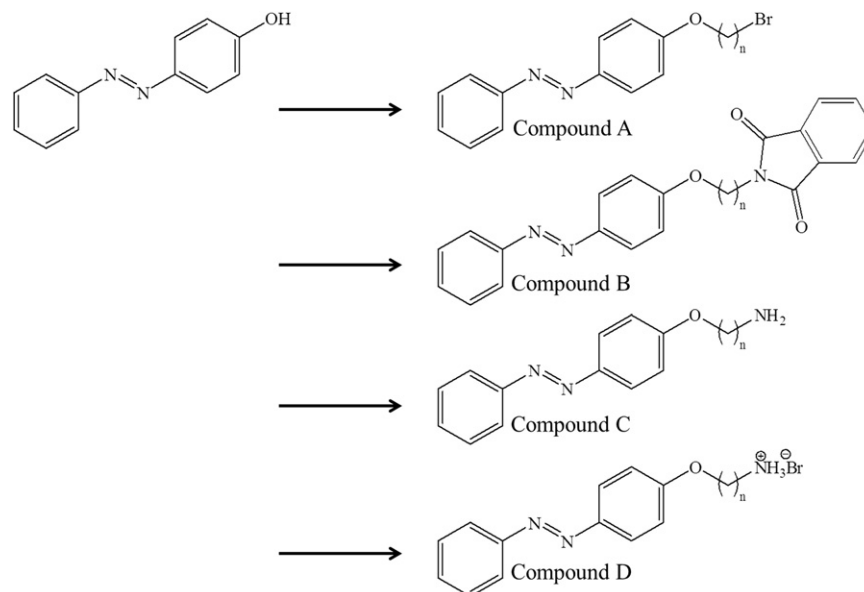
2.2. Synthesis of azobenzene derivatives

The azobenzene derivatives (compound D) used in this study were synthesized according to Scheme 1. Compound A: 4-(phenylazo)phenol (30 mmol) and 1,*n*-dibromoalkane (60 mmol, carbon number: $n=2, 4, 6$) were added to 30 cc of a 1 mol/dm³ NaOH aqueous solution, and then this mixture was refluxed with vigorous stirring overnight. After confirming a neutral pH, the products were extracted by chloroform. After dehydrating the chloroform solution by MgSO₄, compound A as a yellow powder was obtained by evaporating the solvent [$n=2$: yield=76.0%, ¹H NMR (500 MHz, CDCl₃) δ 7.93 (td, 2H), 7.88 (td, 2H), 7.51 (t, 2H), 7.45 (t, 1H), 7.03 (td, 2H), 4.38 (tt, 2H), 3.68 (tt, 2H). $n=4$: yield=38.2%, ¹H NMR (500MHz, CDCl₃) δ 7.92 (td, 2H), 7.88 (td, 2H), 7.50 (tt, 2H), 7.44 (tt, 1H), 7.00 (td, 2H), 4.09 (t, 2H), 3.51 (t, 2H), 2.31–2.08 (m, 2H), 2.02–1.97 (m, 2H). $n=6$: yield=56.4%, ¹H NMR (500 MHz, CDCl₃) δ 7.91 (td, 2H), 7.87 (td, 2H), 7.50 (tt, 2H), 7.43 (tt, 1H), 7.00 (td, 2H), 4.05 (t, 2H), 3.44 (t, 2H), 1.92 (quint, 2H), 1.85 (quint, 2H), 1.54 (quint, 4H)]. Compound B: compound A (15 mmol) and potassium phthalimide (18 mmol) was added to 200 cc of a DMF, and then this mixture was heated at 363 K for 3 h. After evaporating the solvent, the product was extracted by hot water and chloroform, and then the product was rinsed with hot water until bromide ions could no longer be observed by the AgNO₃ method. After dehydrating the chloroform solution by MgSO₄, compound B as an orange powder was obtained by evaporating the solvent [$n=2$: yield=97.6%, ¹H NMR (500 MHz, DMSO-*d*₆) δ 7.90–7.84 (m, 6H), 7.75–7.72 (m, 2H), 7.49 (tt, 2H), 7.43 (tt, 1H), 6.99 (td, 2H), 4.32 (t, 2H), 4.16 (t, 2H). $n=4$: yield=98.5%, ¹H NMR (500 MHz, DMSO-*d*₆) δ 7.91–7.84 (m, 5H), 7.71 (sext, 2H), 7.50 (tt, 2H), 7.43 (tt, 1H), 6.98 (td, 2H), 4.09 (t, 2H), 3.79 (t, 2H), 1.96–1.85 (m, 4H). $n=6$: yield=98.8%, ¹H NMR (500 MHz, DMSO-*d*₆) δ 7.91–7.84 (m, 6H), 7.71 (q, 2H), 7.50 (t, 2H), 6.98 (d, 2H), 4.03 (t, 2H), 3.71 (t, 2H), 1.82 (quint, 2H)]. Compound C: compound B (8 mmol) and

hydrazine monohydrate (400 mmol) was added to 160 cc of a tetrahydrofuran (THF)/ethanol (EtOH) mixed solution (80/20, v/v), and then this mixture was heated at 353 K for 3 h. After removing the white precipitate (phthalic salt), the product was extracted by chloroform. After dehydrating the chloroform solution by MgSO₄, impurities were removed from the concentrated filtrate by diethylether. Compound C as an orange powder was collected by concentrating the obtained filtrate [$n=2$: yield=99.7%, ¹H NMR (500 MHz, CDCl₃) δ 7.92 (d, 2H), 7.88 (d, 2H), 7.50 (t, 2H), 7.44 (t, 1H), 7.03 (d, 2H), 4.09 (t, 2H), 3.13 (t, 2H), 1.53 (br, 2H). $n=4$: yield=68.4%, ¹H NMR (500 MHz, CDCl₃) δ 7.91 (td, 2H), 7.87 (td, 2H), 7.50 (tt, 2H), 7.43 (tt, 1H), 7.00 (td, 2H), 4.07 (t, 2H), 2.80 (t, 2H), 1.88 (quint, 2H), 1.65 (quint, 2H), 1.52 (br, 2H). $n=6$: yield=70.0%]. Compound D: compound C (2 mmol) was added to 100 cc of diethylether under N₂ atmosphere. Hydrobromic acid (2.4 mmol of 47%) was dropped to the mixed solution in an ice bath, producing an orange precipitate. Filtrated compound D as an ochre powder was obtained by a small amount of acetone [$n=2$: yield=99.1%, ¹H NMR (500 MHz, DMS-*d*₆) δ 7.97 (br, 3H), 7.93 (d, 2H), 7.85 (d, 2H), 7.60–7.52 (m, 3H), 7.20 (d, 2H), 4.29 (t, 2H), 3.29 (t, 2H) $n=4$: yield=83.6%, ¹H NMR (500 MHz, DMS-*d*₆) δ 7.90 (td, 2H), 7.84 (td, 2H), 7.68 (br, 3H), 7.58 (tt, 3H), 7.53 (tt, 1H), 7.14 (td, 2H), 4.12 (t, 2H), 2.88 (sext, 2H), 1.82 (quint, 2H), 1.72 (quint, 2H). $n=6$: yield=36.6%, ¹H NMR (500 MHz, DMS-*d*₆) δ 7.89 (td, 2H), 7.84 (td, 2H), 7.63 (br, 3H), 7.58 (tt, 3H), 7.52 (tt, 1H), 7.13 (td, 2H), 4.10 (t, 2H), 2.80 (sext, 2H), 1.77 (quint, 2H), 1.57 (quint, 2H), 1.46 (quint, 2H), 1.39 (quint, 2H)]. Hereafter, synthesized azobenzene derivatives are abbreviated as AzoCnA⁺Br⁻ ($n=2, 4, 6$).

2.3. Preparation of layered perovskite compounds with lead (II) bromide and azobenzene derivatives

AzoCnA⁺Br⁻ (0.10 mmol) and lead(II) bromide (0.05 mmol) were completely dissolved in 0.3 cc of DMF. After irradiating this DMF solution with near UV light (450 nm) for 10 min, precipitates were produced by adding sufficient quantities of acetone to this DMF solution under light shielding. These precipitates were collected by filtration, and then dried under reduced pressure at room temperature. Hereafter, obtained hybrid powders are abbreviated as PbBr-AzoCnA ($n=2, 4, 6$).



Scheme 1. Synthesis routes of AzoCnA ($n=2, 4, \text{and } 6$).

2.4. Photoirradiation of PbBr–AzoCnA powders

To investigate the occurrence of photoisomerization of AzoCnA incorporated in PbBr–AzoCnA hybrids, photoirradiation of PbBr–AzoCnA powder was performed at room temperature. A Xe lamp (300 W: MAX-303, Asahi Spectra Co., Ltd.) was used as the light source. To adjust the wavelength for photoirradiation, band-pass filters for UV irradiation (350 ± 9 nm) and visible irradiation (450 ± 9 nm) were used.

2.5. Characterization

X-ray diffraction (XRD) measurements of PbBr–AzoCnA before and after photoirradiation were performed by powder diffractometer with Ni-filtered Cu $K\alpha$ radiation (50 kV, 100 mA: RINT-2500, RIGAKU). The diffuse reflection (DR) spectra of PbBr–AzoCnA before and after photoirradiation were measured by a V-670 UV–vis spectrophotometer (JASCO, reference sample: MgO powder). The photoluminescence (PL) spectra of PbBr–AzoCnA before and after photoirradiation were measured by FP-6600 fluorophotometer (JASCO) attached to a powder sample holder at an excitation wavelength λ^{ex} of 350 nm at room temperature under ambient conditions. Images of PbBr–AzoCnA powders were captured by a scanning electron microscope (SEM) (JSM-T20, JEOL Ltd.). To identify the chemical situation of the Pb and Br atoms in the inorganic layer before and after photoirradiation, X-ray photoelectron spectroscopy (XPS) was carried out on an ESCA-3300 (Shimadzu) equipped with Al $K\alpha$ radiation. Infrared spectra of PbBr–AzoCnA before and after photoirradiation were measured by the KBr pellet method (FT-IR 6100, JASCO).

The composition formula of PbBr–AzoCnA was determined from the following data: (1) the content of Pb in PbBr–AzoCnA was determined by inductively coupled plasma-atomic electron spectroscopy (ICP-AES: Perkin-Elmer); (2) the abundance molar ratio of Br/Pb in PbBr–AzoCnA was evaluated by scanning electron microscopy–energy dispersive spectroscopy (SEM-EDS: JSM-T20, JEOL Ltd.); (3) the amount of carbon, hydrogen, and nitrogen in PbBr–AzoCnA was evaluated by a CHN corder (MTA-620, Yanaco).

3. Results and discussion

3.1. Preparation of PbBr–AzoCnA hybrid powder

The composition formula of PbBr–AzoCnA hybrid powders calculated from ICP-AES, SEM-EDS, and CHN elemental analysis agreed with the ideal composition formula of PbBr–AzoCnA hybrids, $(Ph-N=N-Ph-O-(CH_2)_n-NH_3)PbBr_4$ (Ph : phenyl group, $n=2, 4, 6$). XRD patterns of all the hybrid powders are shown in Fig. 1. All the hybrid powders exhibited diffraction peaks from the 001 plane, and thus it is found that all the hybrid powders possessed a layered structure. Plate crystals could be observed in the SEM images of all the synthesized hybrid powders (cf. photographs in Fig. 1). These results indicate that PbBr–AzoCnA hybrid materials we wanted to synthesize could be prepared.

In Table 1, both the basal spacing value, d , and the tilt angle, θ , of the major axis of the incorporated AzoCnA molecule against the normal line of the $PbBr_4$ layer are shown. Here, θ values were calculated by using the following equation:

$$\theta = \cos^{-1} \left(\frac{d - 2d_{Pb-Br}}{2L} \right) \quad (1)$$

where d_{Pb-Br} is the thickness of the PbBr layer (0.30 nm) and L is length of the major axis of the AzoCnA molecule with an all-*trans* methylene group. The d values increased with an increase in the n value. However, the θ value, which was about 59° , did not depend on the n value. These facts indicate that synthesized PbBr–AzoCnA hybrid crystals possess the same crystal structure, even when the chain length of the methylene group is varied. Fig. 2 shows the XPS spectra of the (a) Pb 4f and (b) Br 3d orbits of the PbBr–AzoCnA hybrid powders. The position and shape of the peaks originating from the Pb 4f and Br 3d orbits did not change.

Table 1
Basal spacing value, d , and tilt angle, θ , of incorporated AzoCnA molecules.

n	d (nm)	θ (deg.)
2	2.30	58.6
4	2.61	57.8
6	2.88	57.6

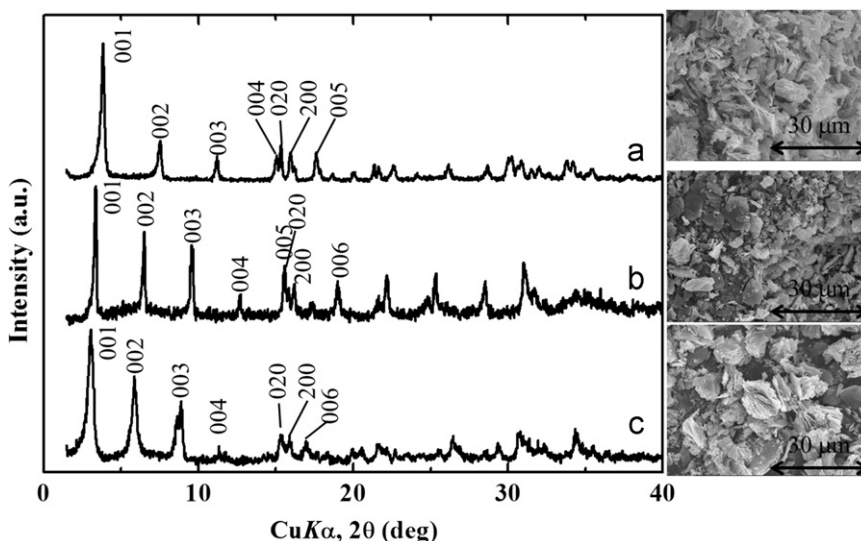


Fig. 1. XRD patterns and SEM images of PbBr–AzoCnA materials [$n=2$ (a), 4 (b), and 6 (c)].

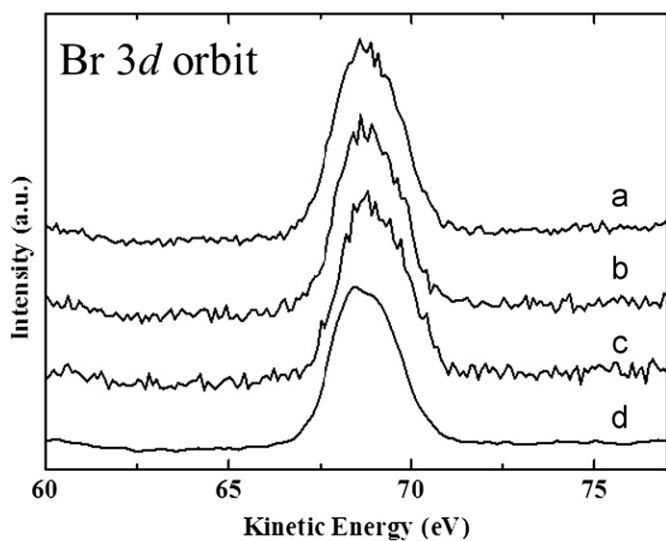
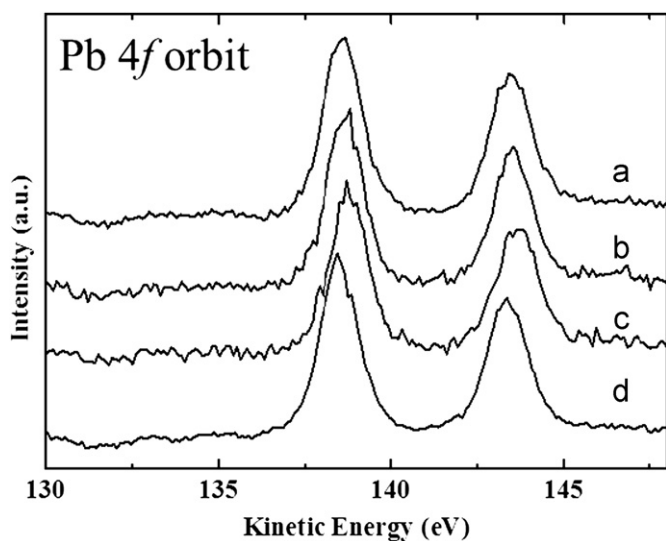


Fig. 2. XPS spectra of Pb 4f (top) and Br 3d (bottom) of PbBr–AzoCnA materials [$n=2$ (a), 4 (b), 6 (c), and $(C_{16}H_{33}NH_3)_2PbBr_4$ (d)].

Moreover, the position and shape of the peaks was the same as that of the $(C_{16}H_{33}NH_3)_2PbBr_4$ hybrid powder, which is a typical hybrid compound. Thus, it is found that the crystal structure of the synthesized PbBr–AzoCnA hybrids is the same as that of the $(C_{16}H_{33}NH_3)_2PbBr_4$ hybrid. The peak originating from the Br 3d orbit was asymmetrical. This is caused by a distortion of the octahedron of $PbBr_4^{2-}$, as reported in previous paper [14]. Thus, we suggest the schematic structure model of PbBr–AzoCnA crystals shown in Fig. 3.

3.2. Spectroscopic properties of PbBr–AzoCnA hybrid powder

Fig. 4 shows the DR and PL spectra of the PbBr–AzoCnA hybrid powders. A new peak or shoulder was observed at around 400 nm in the DR spectra of the PbBr–AzoCnA hybrid powders. Because this peak or shoulder was not observed in the mixed DMF solution of $PbBr_2$ and $AzoCnA^+Br^-$, it is found that this new peak or shoulder appeared by the formation of the hybrid compounds of $PbBr_2$ with $AzoCnA^+Br^-$. Such a peak can also be observed in the DR spectrum of the $(C_{16}H_{33}NH_3)_2PbBr_4$ hybrid powder, and it is well known that this absorption peak is due to the production of excitons in the $PbBr_4^{2-}$ octahedral layer. Thus, it can be expected that excitons in the $PbBr_4^{2-}$ layer of the PbBr–AzoCnA

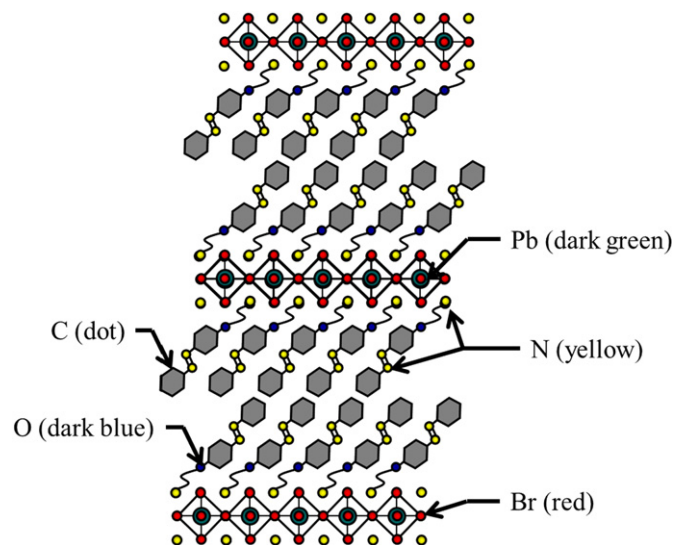


Fig. 3. Schematic model structure of PbBr–AzoCnA hybrid material.

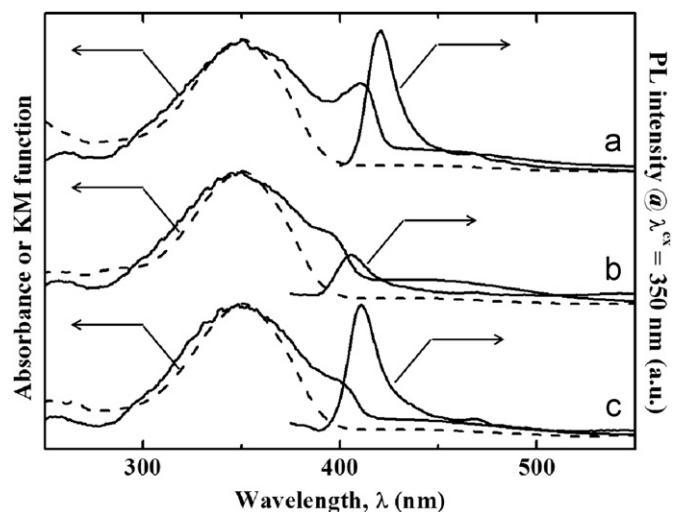


Fig. 4. Photoabsorption and photoluminescence spectra of PbBr–AzoCnA powder (solid lines) and dissolved in DMF solution (broken line) [$n=2$ (a), 4 (b), and 6 (c)].

hybrid compounds will also be produced. Although a mixed DMF solution of $PbBr_2$ and $AzoCnA^+Br^-$ does not show the emission, PbBr–AzoCnA hybrid powders showed a remarkable and sharp PL peak with a small Stokes shift. Thus, it is found that synthesized PbBr–AzoCnA hybrid powders have an objective layered perovskite crystal structure and exhibit PL from excitons produced in the $PbBr_4^{2-}$ layer. Moreover, the absorption peak from the azobenzene group observed around 350 nm did not vary upon hybridization of $PbBr_2$ with $AzoCnA^+Br^-$. This fact indicates that $AzoCnA^+$ cations have no intermolecular interaction in the interlayer space of PbBr–AzoCnA hybrids. Thus, it can be predicted that $AzoCnA^+$ cations in the synthesized PbBr–AzoCnA hybrid powders exhibit a photoisomerization reaction from the *trans*- form to the *cis*- form under UV irradiation.

3.3. Photoisomerization from *trans*- to *cis*-AzoCnA chromophores in PbBr–AzoCnA hybrid powder

Fig. 5 shows the DR spectra of PbBr–AzoCnA hybrid powders before and after UV light irradiation. An absorption peak around 350 nm from the *trans*- form of AzoCnA in all the PbBr–AzoCnA

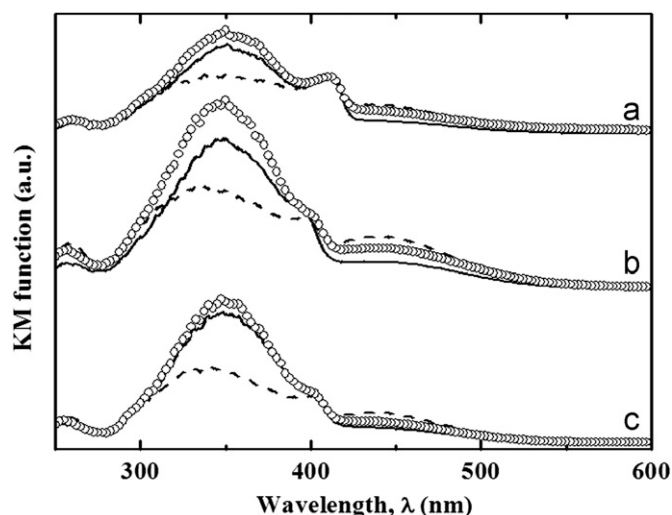


Fig. 5. DR spectra of PbBr–AzoCnA materials [$n=2$ (a), 4 (b), and 6 (c)] before UV irradiation (solid lines), after UV irradiation (broken lines), and after visible irradiation to UV-irradiated samples (circles). (For interpretation of the references to color in this figure legend, the reader is referred to the web version of this article.)

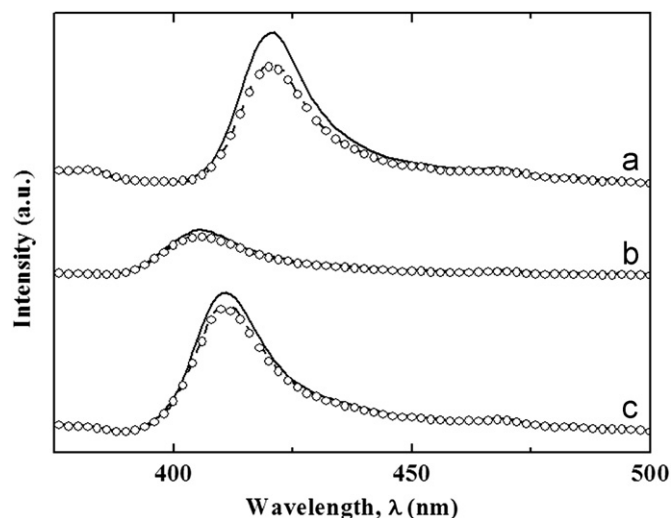


Fig. 6. PL spectra of PbBr–AzoCnA materials [$n=2$ (a), 4 (b), and 6 (c)] before UV irradiation (solid lines), after UV irradiation (broken lines), and after visible irradiation to UV-irradiated samples (circles). (For interpretation of the references to color in this figure legend, the reader is referred to the web version of this article.)

hybrids decreased by UV light irradiation, and then the absorption peak around 450 nm from the *cis*- form of AzoCnA appeared and increased. That is, AzoCnA chromophores incorporated in the PbBr_4^{2-} layer structure exhibited photoisomerization from *trans*- to *cis*- forms under UV light irradiation. Estimating the photoisomerization rate (X) from the *trans*- to the *cis*- forms is determined from the following equation:

$$X = \frac{A_0^{\text{trans}} - A_{\text{ir}}^{\text{trans}}}{A_0^{\text{trans}}} \times 100 \quad (2)$$

where A_0^{trans} and $A_{\text{ir}}^{\text{trans}}$ are the absorbance at 350 nm before and after UV irradiation, respectively. The values of X for PbBr–AzoC2A, PbBr–AzoC4A, and PbBr–AzoC6A were 33%, 32%, and 34%, respectively, and thus were almost same. This fact indicates that the synthesized PbBr–AzoCnA has nearly equal vacant space and can accommodate *cis*- forms of AzoCnA in its interlayer space. Therefore, we succeeded in synthesizing PbBr_4^{2-} -based layered perovskite compounds incorporating AzoCnA chromophores, which, for the first time show a reversible photoisomerization reaction.

Fig. 6 shows the PL spectra of the PbBr–AzoCnA hybrid powder before and after UV light irradiation. The intensity of the PL peak observed around 410 nm decreased under UV light irradiation, regardless of the value of n . The PL spectra of PbBr–C16A did not vary by UV light irradiation. Thus, it is found that this decrease in the intensity of the PL peak is caused by photoisomerization from the *trans*- to the *cis*- forms of AzoCnA chromophores incorporated in the interlayer space of the PbBr_4^{2-} -based layered perovskite compound. Moreover, XRD patterns, FT-IR spectra, morphologies, and XPS spectra of the PbBr–AzoCnA hybrid powders did not change. Fig. 7 shows a structural model of the PbBr–AzoCnA hybrids before and after UV light irradiation as suggested from these experimental results. Thus, the reason why the PL changed by UV light irradiation may have been caused by re-absorption or energy transfer from excitons produced in the PbBr_4^{2-} layers to the *cis*-AzoCnA chromophores. If the reason for reduction of PL intensity by UV light irradiation was re-absorption, then the PL quenching rate is independent of the D values, but if the reason for the reduction was energy transfer, then the PL quenching rate depends on the D values. In Fig. 8, the quenching rates of PL intensity from excitons produced in the PbBr_4^{2-} layers are plotted against distance between the PbBr_4^{2-} layer and the AzoCnA chromophore, D , which shows that PL intensity depends on D value, i.e., PL intensity decreases with an increase in D value. Thus, it is found that this PL quenching can be caused by the energy transfer from excitons produced in the PbBr_4^{2-} layer to the *cis*-AzoCnA chromophore.

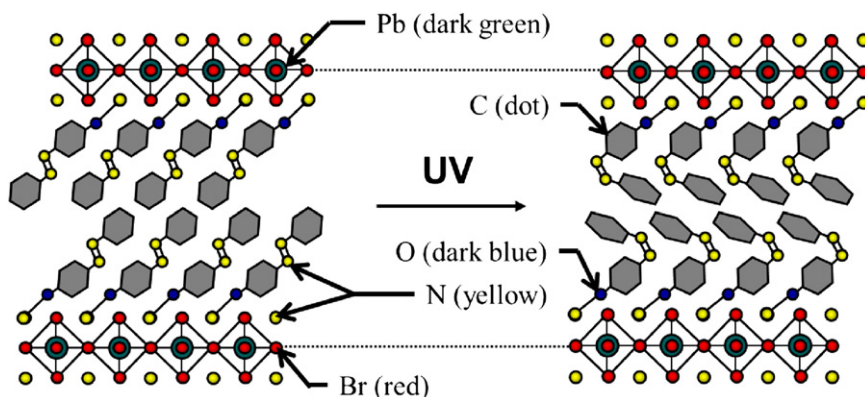


Fig. 7. Schematic model structures of PbBr–AzoCnA hybrid materials before and after UV irradiation.

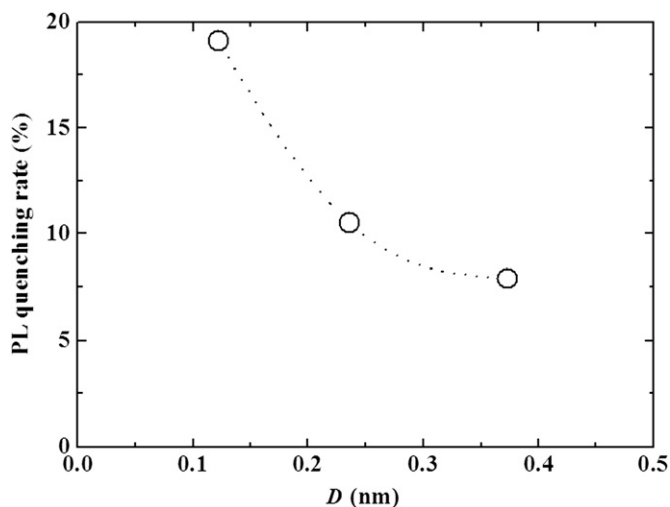


Fig. 8. Dependence of PL quenching rate on D values.

3.4. Iteration photoisomerization reaction of AzoCnA chromophores in PbBr–AzoCnA hybrid powders

In Fig. 9, the intensity of the Kubelka–Munk (KM) function value at the absorption peak of the *trans*- and *cis*- forms of AzoCnA (a) and the PL peak (b) are plotted as functions of iteration number, m . The photo-absorption change of *trans*-AzoCnA observed around 350 nm under both UV and visible light irradiation, which originated from the π - π^* phototransition, was fully reversible regardless of the value of n . However, the KM intensity of *cis*-AzoCnA observed at around 450 nm under both UV and visible light irradiation, which originated from the n - π^* phototransition, gradually increased with an increase in m value. This difference of photoisomerization behavior between *trans*- and *cis*-AzoCnA was abnormal because the photoisomerization behavior of both *trans*- and *cis*-azobenzenes are generally in accord in a dilute solution. Thus, the increase in photoabsorption from the n - π^* phototransition cannot be explained by an increase in the number of *cis*-AzoCnA chromophores. Moreover, the PL intensity of the PbBr–AzoCnA hybrids also decreased with an increase in m value, although the PL intensity was somewhat restored. These results indicate that PL quenching would be caused by the energy transfer from excitons produced in the PbBr₄²⁻ layer to the n - π^* phototransition of AzoCnA chromophores in PbBr–AzoCnA hybrids. The mechanism of the photoabsorption from the n - π^* phototransition of AzoCnA is still unclear, although the self-assembled structure of AzoCnA chromophores in PbBr–AzoCnA hybrids is considered to be one of the reasons of this behavior.

4. Conclusions

In this study, we succeeded in synthesizing hybrid solid materials of AzoCnA chromophores ($n=2, 4, 6$) with PbBr₄²⁻-based perovskite layers, in which for the first time the AzoCnA chromophores exhibited reversible photoisomerization from *trans*- and *cis*- forms. Moreover, the PL intensity of this hybrid material responded to UV and visible light irradiation. Meanwhile, we found abnormal photoisomerization behavior of the AzoCnA chromophores in the PbBr–AzoCnA hybrids, i.e., an increase in the probability of an n - π^* phototransition. However, the reason for this abnormal photoisomerization behavior is unclear and clarification of this abnormal behavior is important in the future work. The present PbBr–AzoCnA hybrid solid

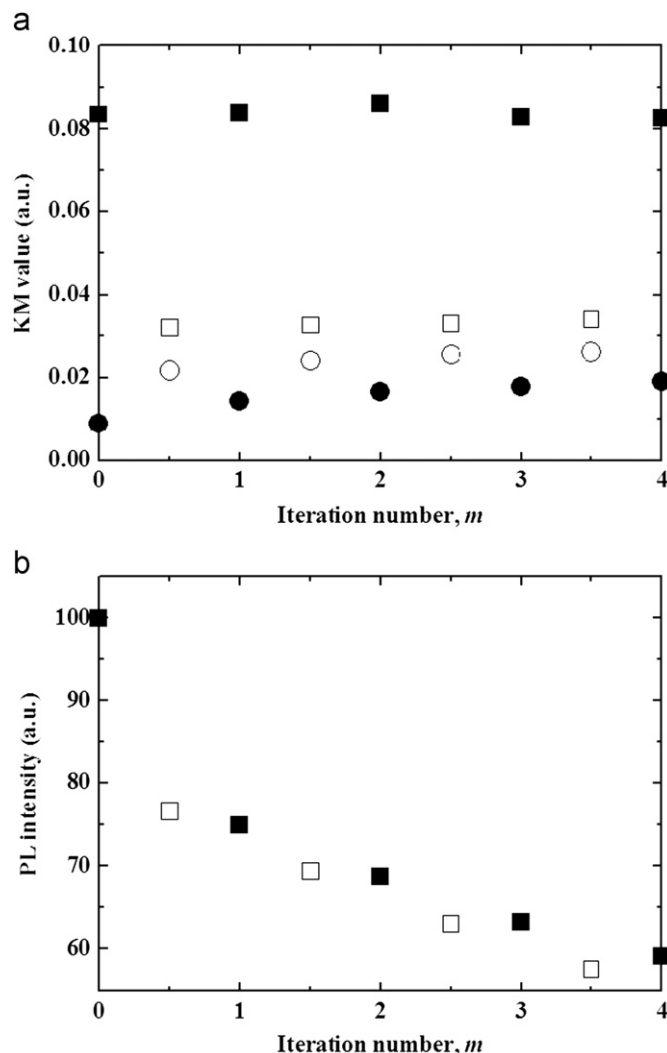


Fig. 9. KM values (a) and PL intensity (b) of PbBr–AzoCnA hybrid materials as a function of iteration number, m , of UV and visible light irradiation.

materials could be recognized as one of the several photoswitchable PL materials, although a way to control the increase in probability of an n - π^* phototransition is required.

Acknowledgments

This work is partly supported by the Research Promotion Foundation of Nagoya University. Authors are grateful to Prof. K. Takase (College of Science and Technology, Nihon University) for fruitful discussions of PL data. The synchrotron-radiation X-ray diffraction experiments for checking the crystallinity of the PbBr–AzoCnA hybrid powder were performed at the BL02B2 in the SPring-8 with approval of the Japan Synchrotron Radiation Research Institute (JASRI) (Program no. 2010A1287).

References

- [1] D.B. Mitzi, J. Mater. Chem. 14 (2004) 2355–2365.
- [2] M. Era, T. Kobayashi, M. Noto, Curr. Appl. Phys. 5 (2005) 67–70.
- [3] N. Kitazawa, Y. Watanabe, J. Phys. Chem. Solids 71 (2010) 797–802.
- [4] N. Kitazawa, M. Aono, Y. Watanabe, J. Phys. Chem. Solids 72 (2011) 1467–1471.
- [5] Y. Li, G. Zheng, J. Lin, Eur. J. Inorg. Chem. 2008 (2008) 1689–1692.
- [6] N. Kitazawa, M. Aono, Y. Watanabe, Thin Solid Films 518 (2010) 3199–3203.

- [7] N. Kitazawa, D. Yaemponga, M. Aono, Y. Watanabe, *J. Lumin.* 129 (2009) 1036–1041.
- [8] M. Era, T. Higashiuchi, K. Yaso, M. Kuramori, Y. Oishi, *Thin Solid Films* 499 (2006) 49–53.
- [9] N. Kitazawa, T. Ito, D. Sakasegawa, Y. Watanabe, *Thin Solid Films* 500 (2006) 133–137.
- [10] M. Sato, M. Yoshizawa-Fujita, Y. Takeoka, M. Rikukawa, *Adv. Mater. Res. Thermec 2011* (2011) S538–S543 (Supplement).
- [11] Y. Takeoka, M. Fukasawa, T. Matsui, K. Kikuchi, M. Rikukawa, K. Sanui, *Chem. Commun.* (2005) 378–380.
- [12] A. Lemmerer, D.G. Billing, *CrystEngComm* 14 (2012) 1954–1966.
- [13] T. Dammak, N. Fourati, H. Boughzala, A. Mlayah, Y. Abid, *J. Lumin.* 127 (2007) 404–408.
- [14] D.B. Mitzi, *J. Solid State Chem.* 145 (1999) 694–704.
- [15] K. Kikuchi, Y. Takeoka, M. Rikukawa, K. Sanui, *Colloids Surf. A* 257–258 (2005) 199–202.
- [16] M. Era, S. Oka, *Thin Solid Films* 376 (2000) 232–235.
- [17] M. Era, A. Shimizu, *Mol. Cryst. Liq. Cryst. Sci. Technol. A* 371 (2001) 199–202.
- [18] T. Ikeda, O. Tsutsumi, *Science* 268 (1995) 1873–1875.
- [19] A. Shishido, O. Tsutsumi, A. Kanazawa, T. Shiono, T. Ikeda, N. Tamai, *J. Am. Chem. Soc.* 119 (1997) 7791–7796.
- [20] H. Sakai, A. Matsumura, S. Yokoyama, T. Saji, M. Abe, *J. Phys. Chem. B* 103 (1999) 10737–10740.
- [21] F. Marlow, K. Hoffmann, J. Caro, *Adv. Mater.* 9 (1997) 567–570.
- [22] S. Kurihara, S. Nomiyama, T. Nonaka, *Chem. Mater.* 12 (2000) 9–12.
- [23] M. Taguchi, K. Yamada, K. Suzuki, O. Sato, Y. Einaga, *Chem. Mater.* 17 (2005) 4554–4559.